# Predicting the Large-Deflection Path of Tapered Cantilever Beams


| Matthew B. Parkinson | Gregory M. Roach | Larry L. Howell |
|---|---|---|
| University of Michigan | Brigham Young University | Brigham Young University |
| 2250 GG Brown Building<br>Ann Arbor, MI 48109-2125<br>734-936-2624<br>734-647-8403 (fax)<br>mparkins@umich.edu | 435 CTB<br>Provo, UT 84602<br>801-378-2019<br>801-378-5037 (fax)<br>roachg@et.byu.edu | 435 CTB<br>Provo, UT 84602<br>801-378-8037<br>801-378-5037 (fax)<br>lhowell@et.byu.edu |



## ABSTRACT

A mathematical model for predicting the deflection path of both non-tapered and continuously tapered cantilever beams loaded with a vertical end force is presented. It is based on the proposition that the path is a function of the ratio of the endpoints' moments of inertia. This was verified through physical testing, comparison to solution of the Bernoulli-Euler equation, and results obtained in finite element analysis. Predicted deflections were found to be accurate within 1.8% of the actual deflection path for moment of inertia ratios varying from 1:1 to 1000:1.


## INTRODUCTION

The deflection path of a cantilever beam (Figure 1) is described by the Bernoulli-Euler equation. This equation is typically simplified and used for small deflection analysis. When the small deflection assumption is inappropriate, costly nonlinear analysis must be performed. For tapered cantilevers, the solution is even more problematic since the resulting differential equation contains variable coefficients.

The elliptic integral solutions for cantilever beams are cumbersome, time consuming, and only usable for simple loading cases. Numerical methods such as nonlinear finite element analysis may also be used to determine the deflection path, but these programs are costly and there is often some difficulty in setting up the proper model. This paper introduces a quick, simplified method for determining the deflection path.

Incremental solutions to this problem exist. Bisshopp and Drucker (1945) posed the non-tapered elliptic integral problem and solved for the deflection using a combination of integral tables and numerical techniques. Flodin (1957) used a modified-graphical method to solve for the deflection path of tapered cantilever beams undergoing small, linear deflections. The large deflection problem was solved numerically by Kemper (1968) for a variety of cases. However, the Runge-Kutta formulation would not converge for some cases and at times required trial and error. Numerical methods were also used by Spolek and Jefferies (1982), who used finite difference to solve for the deflection path of a tapered cantilever with a static transverse end-load. Ohnishi and Matsuzaki (1985) were able to solve for the deflection path of a tapered cantilever beam (a graphite fishing rod) with an applied vertical end-load using non-linear finite element analysis.

In his small-deflection study, Flodin (1957) used the moments of inertia at various points along the beam to scale the deflection values. Similarly, Baumeister and Sebrosky (1972) scaled the moment of inertia at the fixed-end with a parameter that is a function of the ratio of the beam's widths and heights to each other. The method proposed here is a combination of the two. The deflection path is described as an ellipse, with the parameters defining the ellipse determined by beam length and the ratio of the moments of inertia.

## DEFLECTION PATHS

Data sets of deflection paths for beams of varying taper were obtained using a finite element model. These sets were fit with a specific class of second order curve, the ellipse. The coefficients of the ellipses were then made functions of key parameters of the beams (the ratio of the moments of inertia of the ends).

### Finite Element Model

Nonlinear finite element analysis was performed for four cases distinguished by their degree of taper, which was quantified using a ratio of the moments of inertia of the two ends.

$$I_{ratio} = \frac{I_{small}}{I_{big}} \tag{1}$$

The maximum value of the ratio is one (a beam with no taper) and the minimum value approaches zero (a beam that tapers to a point). For practical purposes, a ratio of 1000 to 1, or 0.001 was deemed sufficient for this work. The four cases upon which the predictive model is based were spaced logarithmically: 1, 0.1, 0.01, and 0.001.

A finite element model was constructed using a tapered beam element. One end of the beam was fixed in all degrees of freedom. A vertical displacement was applied to the free end. The beam was deflected until the tip reached an angle of 70° (Figure 1). The *x* and *y* displacements were output for 100 load steps between 0° and 70° of tip rotation.

### CREATING THE MODEL

Examination of the actual deflection paths of several tapered beams showed that the path is nearly elliptical. This realization is critical because it allows the deflection path to be fit with a second-order curve with just a single degree of freedom. Generally, the coefficients *a*, *b*, and *c* must be determined when a second-order curve (i.e. $ax^2 + bx + c$) is fit to data. As demonstrated below, assuming that the path forms an ellipse reduces the problem to the determination of a single coefficient.

The equation for an ellipse is given as

$$\frac{(x - x_0)^2}{a^2} + \frac{(y - y_0)^2}{b^2} = 1 \tag{2}$$

If the center of the ellipse is located at the fixed end of the beam ( 0, 0 ) the equation simplifies to

$$\frac{x^2}{a^2} + \frac{y^2}{b^2} = 1 . \tag{3}$$

With the x-intercept *a* allowed to be the overall length of the beam, *l*, the equation further simplifies to

$$\frac{x^2}{l^2} + \frac{y^2}{b^2} = 1 . \tag{4}$$

The equation can be rewritten for *y* as a function of *x* and *b*

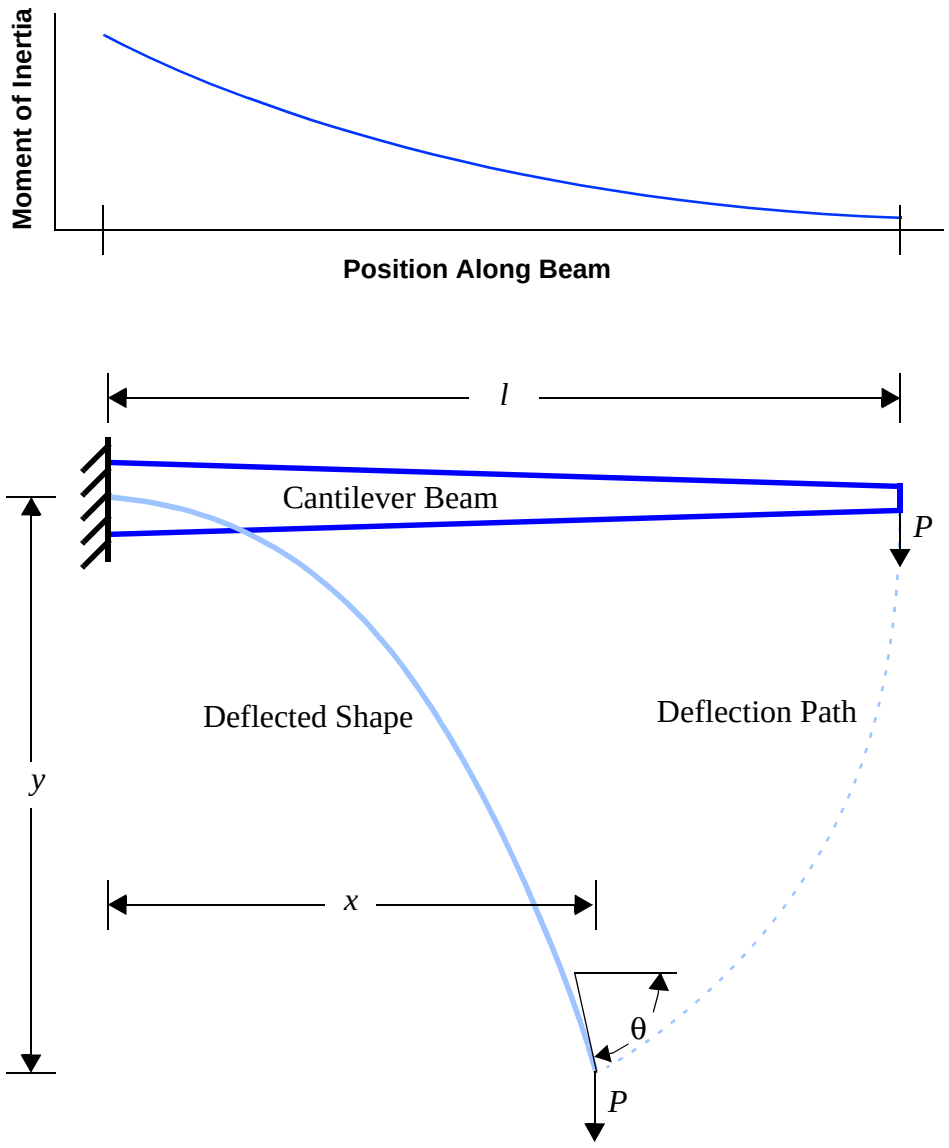


**Figure 1: A diagram detailing the loading and deflection range of the finite element model. Although the beam is linearly tapered, the moment of inertia varies quadratically across the beam.**

$$y = b\sqrt{1 - \frac{x^2}{l^2}} \tag{5}$$

If the value of the y-intercept *b* is known, the *x* and *y* points of deflection can be calculated. The proper value for *b* that produces the ellipse approximating the deflection path must now be determined.

### Calculating "*b*"

The nonlinear finite element analysis produced four sets of data, or deflection paths (Figure 3). An ellipse was fit to each of these. This was done by using an optimization routine to calculate the "*b*" value for each ellipse. The objec-

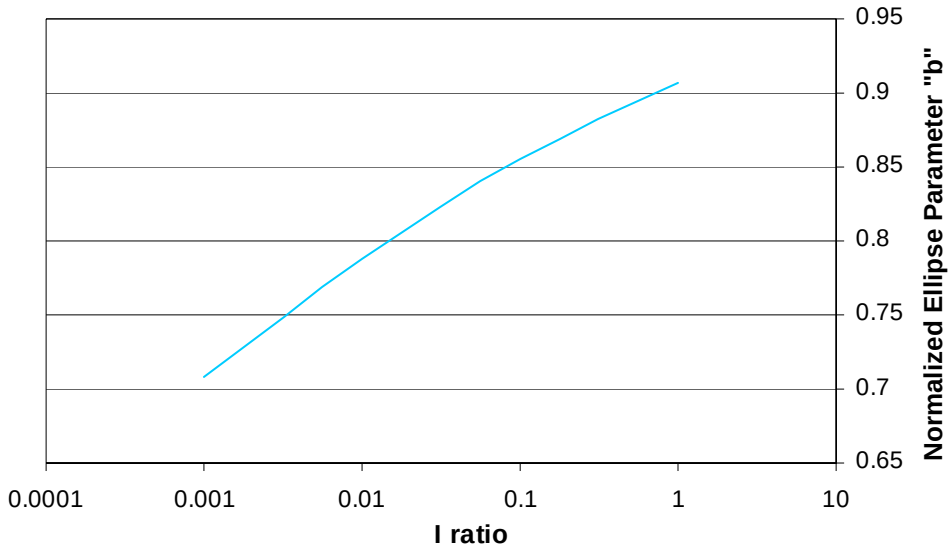


**Figure 2: A log plot of the ratio $I_{small}/I_{big}$ and the normalized ellipse parameter "b"**

tive function, which minimizes the sum of the square of the differences between the finite element data points and those predicted by Equation (5), is then

$$\underset{b}{\text{minimize}} \sum_{i=1}^{100} \left( \hat{y}_i - b\sqrt{1 - \frac{x_i^2}{l^2}} \right)^2 \tag{6}$$

The percentage of error was calculated using the following equation for each of the data points in the set.

$$\text{error \%} = \left| \frac{\hat{y} - y}{\hat{y}} \right| \tag{7}$$

The maximum percentage error for each path is summarized in Table 1. The closeness of the approximation corroborates the decision to use the ellipse as the basis for the model.

The ellipse parameter *b* was normalized by dividing it by the undeflected length of the beam. This normalized value was then correlated with the ratios of the moments of inertia for the four cases. Figure 2 which presents this

**Table 1: Individual Model Results**

| Ratio $I_{small}/I_{big}$ | 1.0 | 0.1 | 0.01 | 0.001 |
|---|---|---|---|---|
| Max Error % | 0.70 | 0.38 | 0.63 | 1.73 |
| Avg. Error % | 0.41 | 0.19 | 0.33 | 1.09 |

data on a log plot, shows the near linearity of this relationship.

Knowing that the relationship between the natural log of the $I_{ratio}$ and the parameter *b* is almost linear suggests that the previous prediction equation, Equation (5), can be modified by replacing *b* with the equation for a line. This yields Equation (8).

$$y = (c_1 \ln I_{ratio} + c_2) l \sqrt{1 - \frac{x^2}{l^2}} \tag{8}$$

The optimization problem used previously to determine the *b* values can now be modified to find the coefficients of the linear fit. In an effort to increase the accuracy of the model, the scope of the objective function is also modified to include all four data sets simultaneously rather than individually. To give equal weight to each of the data sets, the error must be measured in a new way. Rather than minimizing the sum of the square of the differences, the objective is to minimize the maximum percentage of error within the model. These modifications result in the new formulation of the unconstrained optimization problem

$$\underset{c_1, c_2}{\text{minimize}} \max_{i = 1 \ldots 4} \left\{ \max_{j = 1 \ldots 100} \left\{ \left| \frac{\hat{y}_{i,j} - (c_1 \ln(I_{ratio_j} + c_2))\, l_i \sqrt{1 - \frac{x_{i,j}^2}{l_i^2}}}{\hat{y}_{i,j}} \right| \right\} \right\} \tag{9}$$

As expected, the results (summarized in Table 2) of this second optimization are not as accurate as those obtained in the first, when each data set is fit with its own ellipse. The results are, however, accurate enough for practical use and they justify the assumption of a linear relationship between $I_{small}/I_{big}$ and the ellipse parameter *b*. Figure 3, shows the actual and predicted deflection paths for the four cases.

The final prediction equation, which gives the deflection as a function of the beam length and the ratio of the moments of inertia of the two ends, is then

$$y = (0.030432 \ln I_{ratio} + 0.91897) l \sqrt{1 - \frac{x^2}{l^2}} \tag{10}$$

**Table 2: Global Model Results**

$c_1$ = .030432, $c_2$ = .91897E

| Ratio | 1.0 | 0.1 | 0.01 | 0.001 |
|---|---|---|---|---|
| Max Error % | 1.78 | 1.17 | 1.78 | 1.78 |
| Avg. Error % | 1.06 | 0.94 | 0.93 | 1.12 |

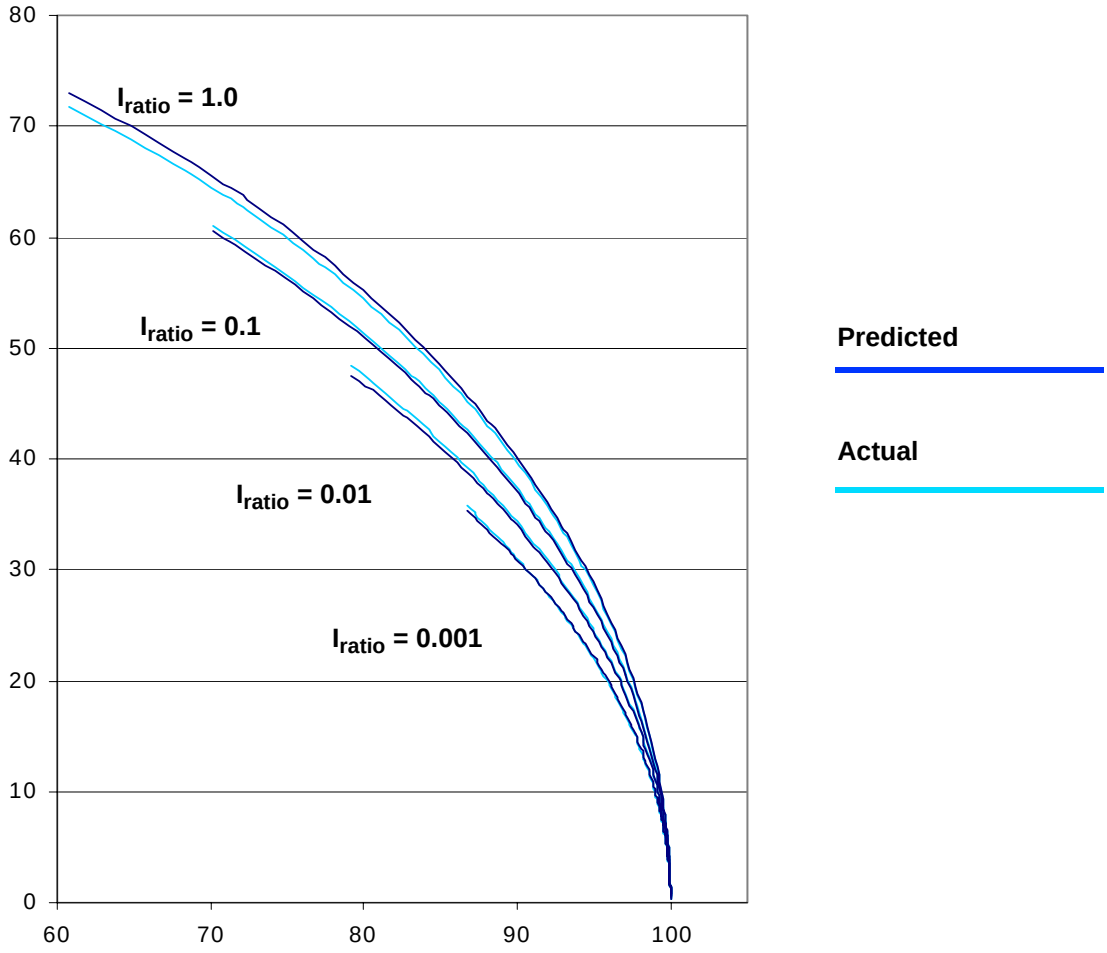


**Figure 3: The actual and predicted deflection paths for the four developmental cases**

## VALIDATION

The model was created using data sets of four $I_{ratios}$ representing the breadth of the area of interest. The following sections test the accuracy of the model by comparing deflection paths predicted by the model against "actual" paths given by experimentation, the Bernoulli-Euler equation, and nonlinear finite element analysis. $I_{ratios}$ were chosen to be different than, but within the bounds of, those selected to build the model.

### Bernoulli-Euler Validation

As a second test of the model, its results were compared against those obtained by the numerical solution of the Bernoulli-Euler equation. This example investigates one extreme of the model's range: a non-tapered beam ($I_{ratio}$ = 1.0). The profile, cross-section, and physical properties are summarized in Figure 4. Substituting into Equation (10) gives

$$y = 0.9190\sqrt{1-x^2} \tag{11}$$

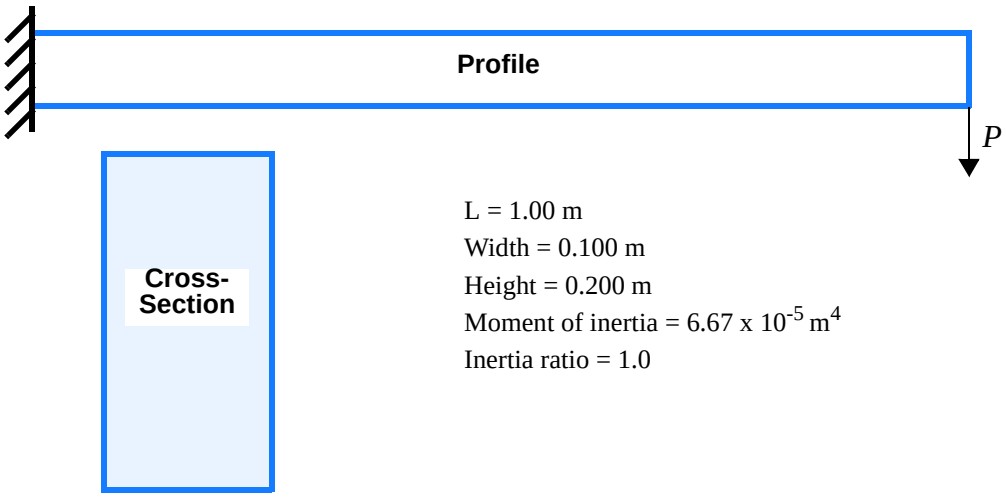


**Figure 4: Physical properties of the polypropylene beam**

To use the Bernoulli-Euler equation, material and geometric properties and loading conditions are required. The cantilever beam was loaded only in the y-direction. The loads were incrementally increased until the tip angle measured 50°. Path coordinates at each of the positions were recorded. The results from the Bernoulli-Euler equation and those predicted by Equation (11) are in Table 3.

### Physical Test

The second validation test examines the other extreme case: taper to a near-point. It involves the physical deflection of a flyrod blank. These are made of graphite and have a continuous taper from butt to tip. Typically, the $I_{ratio}$ is ~0.003, which is within the scope of this model. A profile and cross-section of the blank used for this test as well as specific material properties are in Figure 5.

For this example, the deflection path was determined by mounting the rod horizontally in a machining collett block. The block was clamped to a marking board that was covered with a 3.175 square mm grid. Weights were suspended from the end of the beam and the corresponding point of deflection was marked on the grid to determine the actual deflection path of the beam.

The predicted deflection path, obtained from the physical properties of the blank and Equation (10), is

$$y = 0.9864\sqrt{1 - \frac{x^2}{1.732}} \tag{12}$$

**Table 3: Bernoulli-Euler Test Results**

| | | | | | | |
|---|---|---|---|---|---|---|
| x (m) | 0.988 | 0.974 | 0.956 | 0.913 | 0.867 | 0.822 |
| $y_{actual}$ (m) | 0.142 | 0.208 | 0.268 | 0.372 | 0.454 | 0.517 |
| $y_{pred}$ (m) | 0.143 | 0.209 | 0.271 | 0.376 | 0.459 | 0.524 |
| error % | 0.781 | 0.756 | 0.928 | 0.973 | 1.15 | 1.32 |

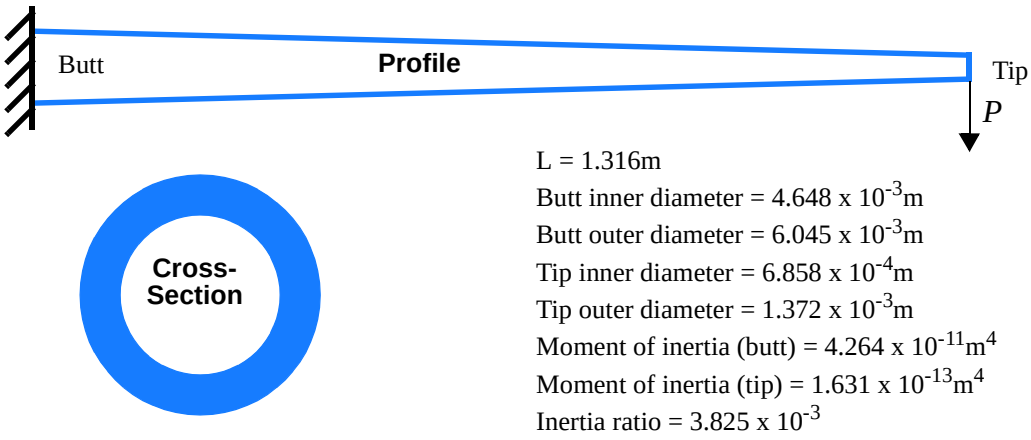


**Figure 5: Physical properties of the tip section of a G. Loomis 9 foot, 5 weight GLX flyrod**

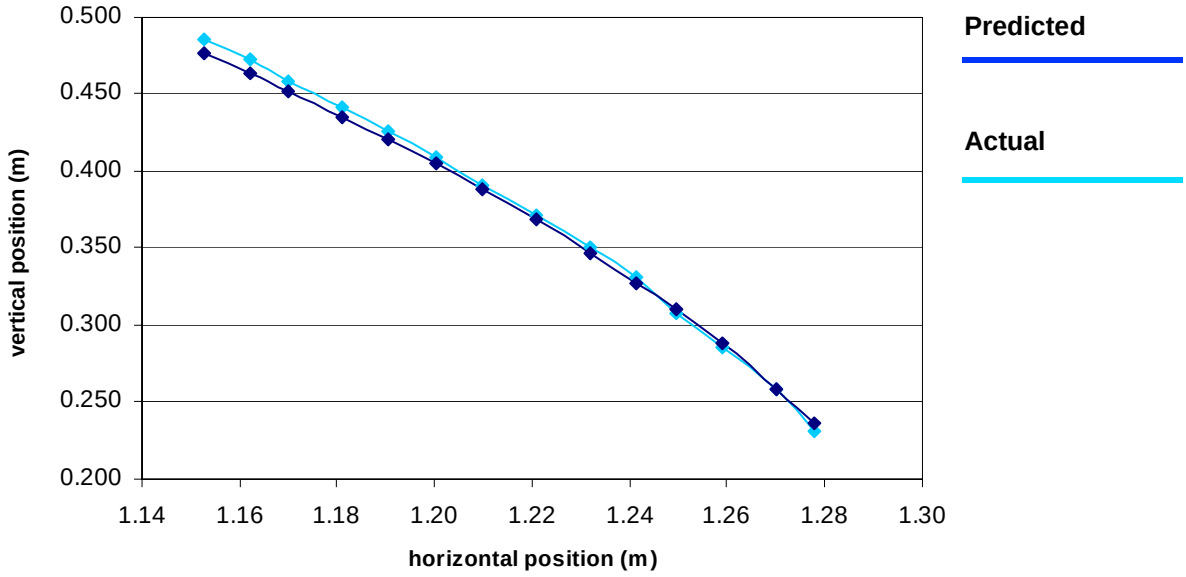


**Figure 6: Predicted and Actual deflection path for Tapered Composite beam**

The measured data and the path predicted by Equation (12) are plotted in Figure 6. The predicted data differs from the actual data by less than 2.05%, as seen in Table 4. The scattered nature of the error distribution is due to inaccuracies in the measured values. In general, the model does quite well and the results are within the accuracy suggested in its development. Note that despite radical differences between this example, the cases used to develop the model, and the previous example, each deflection path is represented accurately.

### Morphed Rectangle

As a final example, consider the beam whose cross-section is a vertical rectangle on one end and a horizontal rectangle on the other (Figure 7), the beam tapering continuously between them. Although the shape of the cross-sec-

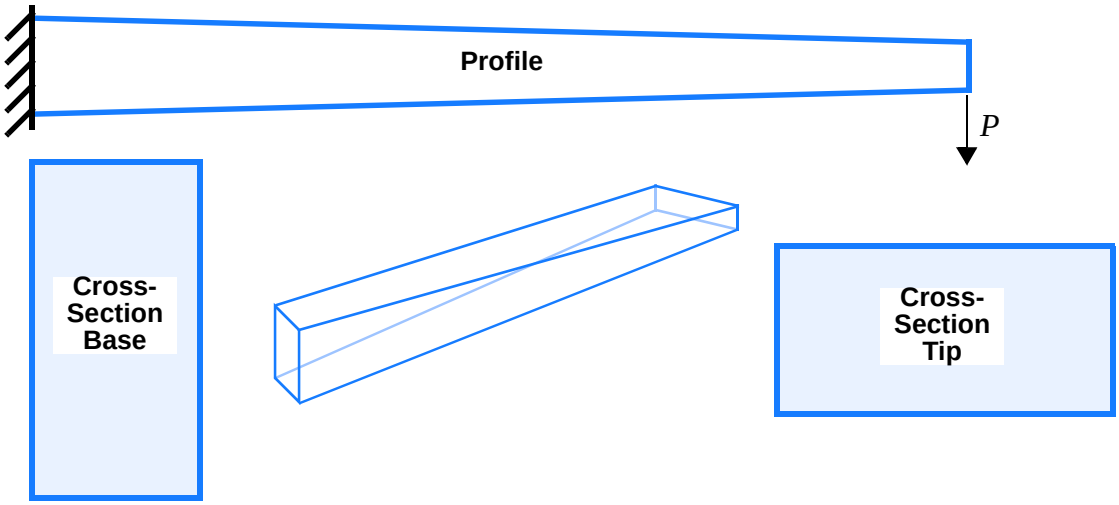


L = 1.00 m
Base width = 0.050 m
Base height = 0.100 m
Base moment of inertia = 4.167 x $10^{-6}$ $m^4$
Tip width = 0.100 m
Tip height = 0.050 m
Tip moment of inertia = 1.042 x $10^{-6}$ $m^4$
Inertia ratio = 0.25

**Figure 7: Physical properties and geometry of the morphed-rectangle beam**

tion is constantly changing and the geometry is quite different from the previous examples, the moment of inertia does continuously taper from the base to the tip. Since this is the case, the model should predict the deflection of this beam as accurately as it has the previous examples.

Given an $I_{ratio}$ of 0.25 and a beam length of 1.0, the equation predicting the deflection path is

$$y = 0.8768\sqrt{1-x^2} \tag{13}$$

Nonlinear finite element analysis was performed on a solid model of the beam. The base (the left end of the

**Table 4: Physical Validation Test Results**

| x (m) | 1.28 | 1.27 | 1.26 | 1.25 | 1.24 | 1.23 | 1.22 | 1.21 | 1.20 | 1.19 | 1.18 | 1.17 | 1.16 | 1.15 |
|---|---|---|---|---|---|---|---|---|---|---|---|---|---|---|
| $y_{actual}$ (x$10^{-1}$m) | 2.32 | 2.59 | 2.86 | 3.08 | 3.32 | 3.51 | 3.71 | 3.91 | 4.10 | 4.25 | 4.41 | 4.59 | 4.73 | 4.86 |
| $y_{pred}$ (x$10^{-1}$m) | 2.36 | 2.59 | 2.88 | 3.10 | 3.28 | 3.47 | 3.69 | 3.89 | 4.05 | 4.21 | 4.35 | 4.52 | 4.63 | 4.77 |
| error % | 1.71 | 0 | 0.68 | 0.72 | 1.25 | 1.01 | 0.74 | 0.45 | 1.10 | 1.14 | 1.33 | 1.48 | 2.05 | 1.89 |

beam) was fixed in all degrees of freedom and a vertical deflection load was applied at the tip. The *x* locations for varying applied *y* deflections of the beam tip were recorded. These are summarized in Table 5, where they are compared with those predicted by Equation (13).

As predicted, the model is also accurate for this case. The largest error being 1.44% over the large deflection path.

## CONCLUSION

The path traced by the tip of a continuously tapered beam undergoing large deflection is a function of the ratio of the moments of inertia of the endpoints. This path can be described as an ellipse. Using the data from several carefully chosen deflections, the equation for this ellipse, as a function of the ratio of the moments of inertia, was found. Based upon these data and three other validation strategies, including comparison against the Bernoulli-Euler equation and physical experimentation, this model is believed accurate within 1.8% through 70 degrees of deflection.

In circumstances where the small deflection assumption is inappropriate, nonlinear finite-element analysis or an elliptic integral solution is typically required. This is particularly costly when the beam is tapered or the geometry is complicated. In such circumstances, the model developed here may be sufficiently accurate and is extremely easy to use.

## ACKNOWLEDGEMENTS

The help of Brent Weight in gathering experimental data is gratefully acknowledged. The donation of materials from Orvis, Sage, Lamiglas, St. Croix, and G. Loomis fly rod manufactures is also acknowledged. This work is supported by the National Science Foundation (NSF) under an NSF CAREER Award under grant No. DMI-9624574.

**Table 5: Morphed Rectangle Test Results**

| | | | | | | | |
|---|---|---|---|---|---|---|---|
| x (m) | 0.9857 | 0.9596 | 0.9190 | 0.8615 | 0.7835 | 0.6785 | 0.5376 |
| $y_{FEA}$(m) | 0.1500 | 0.2500 | 0.3500 | 0.4500 | 0.5500 | 0.6500 | 0.7500 |
| $y_{pred}$ (m) | 0.1478 | 0.2466 | 0.3457 | 0.4451 | 0.5449 | 0.6441 | 0.7393 |
| difference % | 1.4440 | 1.3613 | 1.2296 | 1.0802 | 0.9363 | 0.9132 | 1.4295 |

## REFERENCES

Baumeister, H.K. and Sebrosky, R.A., 1972, “Deflection and Slope in Tapered Beams,” *Machine Design*, Vol. 44, pp. 65-67.

Bisshopp, K.E. and Drucker, D.C., 1945, “Large Deflections of Cantilever Beams,” *Q. Applied Mathematics*, Vol. 3, pp. 272-275.

Flodin, J., 1957, “Deflection of Beams of Varying Moments of Inertia,” *J. of American Society of Nautical Engineers*, Vol. 69, pp. 511-514.

Kemper, J.D., 1968, “Large Deflections of Tapered Cantilever Beams,” *International Journal of Mechanical Science*, Vol. 10, pp. 469-478.

Ohnishi, H. and Matsuzaki, A., 1985, “The Large Deformation Analysis of a Graphite Fishing Rod,” *Computers & Structures*, Vol. 21, No. 1/2, pp. 265-271.

Spolek, G.A. and Jefferies, S.R., 1982, “Analysis of Large Deflections of Fishing Rods,” *Proceedings of the International Conference on Computational Methods and Experimental Measurements*, Washington D.C., pp. 637-648.